

A Ground Truth Bleed-Through Document Image Database

Róisín Rowley-Brooke, François Pitié, and Anil Kokaram

Department of Electronic and Electrical Engineering,
Trinity College Dublin, Ireland
`{rowleybr,fpitie,anil.kokaram}@tcd.ie`

Abstract. This paper introduces a new database of 25 recto/verso image pairs from documents suffering from bleed-through degradation, together with manually created foreground text masks. The structure and creation of the database is described, and three bleed-through restoration methods are compared in two ways; visually, and quantitatively using the ground truth masks.

Keywords: Document database, bleed-through, document restoration

1 Introduction

Bleed-through degradation poses one of the most difficult problems in document restoration. It occurs where ink has seeped through from one side of the page and interferes with text on the other side. There have been many proposed solutions to the bleed-through problem, and it is clear that researchers working in the area of bleed-through restoration are faced with two main challenges. Firstly, it can be difficult to obtain access to high resolution degraded images unless connected with a specific library or digitisation project. Secondly, for all document restoration techniques, problems arise when trying to analyse results quantitatively, as there is no actual ground truth available. This problem may be overcome either by creating synthetic degraded images with known ground truth, [5],[16], or by creating synthetic ground truth data for given real degraded images, [2]. Alternatively, performance may be evaluated without any ground truth by quantifying how the restoration affects a secondary step, such as the performance of an Optical Character Recognition (OCR) system on the document image, [17],[16]. A further issue with quantitative evaluations for performance comparison is that results of different methods are often in different formats, such as binary images [1], pseudo-binary images where the background is uniform with varying foreground intensities [10],[8], or a textured background medium with varying foreground and background intensities [17],[11]. We propose that a fair quantitative comparison between methods can only be achieved if they are converted to the same format then compared to a ground truth that is also of the same format, and the simplest way of achieving this is to binarise all the results and compare them to a binary ground truth. To our knowledge there

are no bleed-through datasets with ground truth freely available for researchers at this time. Since converting scanned manuscript images to a suitable format for use in bleed-through restoration algorithms can be a time consuming process, we hope that the database introduced here, where all necessary processing has been done already, will prove to be a very convenient tool.

The contributions of this work are: (i) A Document Bleed-Through Database, containing 25 recto/verso image pairs, and manually created foreground text ground truth masks. (ii) A quantitative comparison method for results of different manuscript restoration algorithms, where the results are converted to a comparable format and ranked based on probability error metrics.

Section 2 contains the details of the database. Section 3 describes the bleed-through problem, and the chosen restoration techniques. In Section 4 the implementation is described and results are presented, and then discussed in Section 5. Finally the conclusions are presented in Section 6.

2 The Database

A new bleed-through document image database has been compiled for this work, consisting of 25 registered recto/verso image pairs, taken as crops from larger manuscript images with varied degrees of bleed-through degradation. The average crop size is 573x2385 pixels. All images contained in the database are taken from the collections of the Irish Script On Screen Project (ISOS).¹ ISOS is a project of the School of Celtic Studies, Dublin Institute for Advanced Studies, Dublin, Ireland, and is funded by the Dublin Institute for Advanced Studies.² The object of ISOS is to create digital images of manuscripts written in Irish, and to make these images accessible as an electronic resource for researchers.

Image Capture. Each manuscript image was scanned at 600dpi, and also photographed. The images used for the database were the photographs, taken using a 5x4 format viewing camera with a Phase One P45 digital back. Both camera and manuscript were positioned on a specially adapted book-cradle. Each image was processed in Photoshop to crop to an optimum canvas size and superimposes a text header and footer to distinguish each page. A ruler was also placed alongside each image to indicate scale. Digital enhancement was not performed at this stage.

Crop Details. As mentioned in Section 1 some pre-processing is necessary to crop out binding, ruler markers, and digital labels that could influence the performance of intensity based algorithms. Also, as high resolution manuscript images are often very large in size it is not practical to use them for testing - smaller sections are preferable. For the database crops were taken from the larger images such that they would contain a sentence or phrase of text on both the recto and

¹ <http://www.isos.dias.ie>

² <http://www.dias.ie>

verso sides. The reason for this was to allow for the possibility of restoration evaluation using legibility improvement as a metric. All the images were converted to grayscale and saved in tif format. File names in the database follow the format “lib”.“MS”.“fol”.tif. “lib” represents the library from which the manuscript contained in the image originates and can be one of eight labels: (i) AC - The Allan and Maria Myers Academic Centre, University of Melbourne, Australia. (ii) FH - The Benjamin Iveagh Library, Farmleigh House, Ireland. (iii) NLI - The National Library of Ireland. (iv) NUIG - The James Hardiman Library, National University of Ireland, Galway. (v) NUIM - The Russell Library, National University of Ireland, Maynooth. (vi) RIA - The Royal Irish Academy Library. (vii) TCD - Trinity College Dublin Library. (viii) UCD - University College Dublin Library. “MS” refers to the manuscript number (eg. “MS1333”), and “fol” refers to either the page number, or the folio number followed by “r” or “v” to denote the recto or verso side. The ground truth images are labelled as for the degraded images, but with appended “gt.tif” to differentiate between the two.

Registration. To perform non-blind bleed-through restoration (see Section 3), the recto and verso sides must first be registered so that the bleed-through interference on both sides is aligned with its originating text from the opposite side. The registration method used involved three stages. Firstly a set of corresponding control points on both recto and verso images were manually selected. These points indicated locations of the same textual features on each side. A global affine warp model was then derived from a least squares fit to the displacements between these locations. Secondly, this affine model was used as an initialisation to the affine warp optimisation method of Dubois et al. [4]. Finally, local adjustments were made to the registration manually, using the ‘gridwarp’ function in NUKE,³ that defines a grid over the source image, and allows the user to reposition the corners of squares in the grid, warping the local image region correspondingly. Some difficulties were encountered in registration of images where the crops contained text close to the manuscript binding. In these regions the page deformation is nonlinear and an affine model is unsuitable. This problem was overcome by using manual registration only, with a very fine grid over the whole image.

Ground Truth Creation. The ground truth foreground images were created manually, by drawing around the outline of foreground text on both recto and verso sides. These outline layers were then extracted from the images and filled in to create binary foreground text images, with black representing text, and white representing background. In handwritten documents, the edges of characters can often be blurred or gradually fade into the background due to ink absorption by the medium, or due to the angle and pressure of the writing instrument. This makes marking the precise location of the boundary between text and background a very subjective decision. For all the images it was decided that the

³ The Foundry’s node-based compositor, <http://www.thefoundry.co.uk/products/nuke>

edge of characters would be defined where the last traces of ink were visible when viewed in close detail, as it was considered preferable to preserve as much of the foreground text shape as possible.

Those wishing to access the database should contact Róisín Rowley-Brooke at the email address listed above, alternatively information on accessing the database may be found at:

<http://www.isos.dias.ie/libraries/Sigmedia/english/index.html>

3 Bleed-Through Removal

Approaches to bleed-through restoration can be separated into two categories according to whether both sides of the document are used - non-blind methods - or one side only - blind methods. In the case of non-blind methods, there is clearly more information available to work with, however, registration is an essential pre-processing step that can pose many challenges, (see Section 2). Furthermore, there may only be an image of one side of the page available. Conversely, for blind methods registration is not necessary, but there is less image data available to work with.

Blind Methods. Blind methods are mostly based on the assumption that there are three distinct intensity groups in the degraded images - the darkest region corresponding to foreground, the brightest to background, and bleed-through somewhere in between. There are many approaches available for segmentation based on intensity, for example, hysteresis thresholding [5], iterative K-means clustering and principle component analysis (PCA) [3], independent component analysis (ICA), either on the colour channels [15], or different colour space images [14]. However, the main issue with using intensity information only is that this will not be sufficient in severe cases where the bleed-through is equivalent in intensity to the foreground text. In these cases some spatial information is needed. Wolf in [17] uses intensity based clustering initially, then includes spatial information in the form of smoothness priors for the estimated recto and verso hidden label fields, modelling the problem via a dual-layer Markov Random Field (MRF).

Non-Blind Methods. Many non-blind methods use comparative intensity information from both sides to improve the performance of thresholding and segmentation algorithms. For example Sauvola's adaptive thresholding algorithm [12] followed by fuzzy classification is used in [2], the Kullback-Leibler (KL) thresholding algorithm and the binarisation algorithm of Gatos et al. [6] are extended by adding in second threshold levels for the bleed-through interference in [1], and ICA is extended to double-sided documents in [16], using the recto and the flipped verso images as the sources. A model based approach is used in [9], where a function of the *difference* in intensities between the two sides is used to locate bleed-through regions. Physical diffusion-based models are defined for the foreground text, bleed-through interference, and the background medium, and

then a reverse diffusion model is applied on bleed-through regions to remove interference.

Selected Methods. Three recent non-blind techniques that use both spatial and intensity information were chosen to test on the database. Firstly the method for bleed-through reduction proposed by Huang et al. in [7] and [8], (referred to as *Huang*), aims to classify pixels as foreground, background, or bleed-through based on the *ratio* of intensities between the recto and verso sides, and spatial smoothness is enforced in a dual-layer MRF framework. The data cost energy is defined from a small set of user input training data, in the form of coloured strokes drawn by the user in the regions of each pixel class on both sides. These data are then used to define the energy via K-Nearest Neighbour (KNN) and Support Vector Machine (SVM) classification of the intensity ratios. An intra-field prior energy is used to ensure spatial smoothness in the classification of each layer, but also an inter-field prior ensures that certain label combinations between layers cannot occur, such as bleed-through in the same location on both sides. The energy is minimised using graph cuts, and areas classified as background or bleed-through are replaced with the mean background intensity value.

Secondly Moghaddam and Cheriet incorporated the diffusion model idea in [9] to a unified framework in [10], (referred to as *Mogh*), using variational models for non-blind and blind bleed-through removal. Their double-sided wavelet method uses, again, a function of the *difference* in intensity between the degraded recto and verso sides as an indicator of bleed-through and foreground text regions, and spatial smoothness is enforced in the wavelet domain. The variational model for each side consists of three terms: a ‘fidelity’ term ensures the restored image is close to the original in foreground regions, and a ‘reverse diffusion’ term ensures the restored image is close to a uniform target background in background and bleed-through regions. These two terms are weighted by the function of the intensity difference. The third component of the model is the smoothness term, defined on the wavelet coefficients of the restored image, with a smoothing parameter λ chosen based on the estimated background of the degraded image. The smoothing term ensures that the restored image does not contain harsh cut-off at character edges and that fine details are preserved. The solution of the model is obtained using hard wavelet shrinkage.

Finally, in our previous work, (referred to as *RB*) [11], we proposed a method that is based on a linear additive mixing model for the degraded images. However, binary foreground masks are included in the model explicitly to limit the presence of bleed-through to certain regions only. The intensity information on each side is used to define the masks initially, via K-means clustering (the darkest of three clusters representing an estimate of foreground text). Spatial smoothness is enforced in a dual-layer framework, similar to [17] and [7], but instead of solving for a binary or ternary labelling, the clean images intensities themselves are estimated using the degradation model. Intra-layer smoothness priors are used for the masks and mixing parameters on each side, and an inter-layer prior is also used for the mixing parameters to ensure that bleed-through cannot occur in the

same location on both sides. Estimates for the model parameters are obtained via a variation of Iterated Conditional Modes (ICM). A secondary linear model without limiting masks is substituted every 10 iterations for the clean image estimates to ensure that the resulting clean images appear smooth with minimal visible bleed-through artefacts remaining.

4 Results

The implementation details and results of three chosen non-blind methods are presented in what follows. For the *Huang* implementation user markup consisted of 9 – 12 strokes drawn on both recto and verso sides. For some image pairs the recto or verso side were classed entirely as background, or background and bleed-through with no foreground. The result was therefore an image of constant mean background intensity. In these cases the markup was repeated with a greater amount of strokes highlighting the foreground regions until a visually good classification was achieved. In the case of *Mogh* also the restoration results were not optimal on some images; the smoothing parameter, λ , estimate in these instances was too low. However, unlike in the *Huang* results, this did not affect detrimentally the legibility of the resulting image. For these images therefore two versions of the *Mogh* results were examined, the results with the automatically selected λ , and a result where the value of λ was chosen manually to produce the best result visually. For *RB* implementation, the restoration was performed over 35 iterations for each image pair, with the alternative linear model for the clean images substituted four times - at iterations 10, 20, 30, and 35.

Visual Comparison. Some examples of results of the three methods on documents with different degrees of bleed-through degradation are shown in what follows. Fig. 1 shows results on three recto sides of documents with varied bleed-through degradations. The first group shows a document with light bleed-through and clear distinction in intensity between foreground and bleed-through texts. The extract is taken from a 16th Century Irish Primer in The Benjamin Iveagh Library, Farmleigh House, by kind permission of the Governors and Guardians of Marshs Library, Ireland. The top image shows the original degraded recto and then subsequent images show results using *Huang*, *Mogh*, and *RB* respectively. In the right hand column example, the degradation is more pronounced, and there is less distinction between foreground and bleed-through texts. The extract is from a 16th Century collection of Ossianic tales and poems in Irish, courtesy of the National Library of Ireland. The order of results is the same as for the light bleed-through. Finally, the bottom left shows results on a very severe example, where the foreground and bleed-through text intensities are indistinguishable. This extract is taken from a 17th Century *Foras Feasa ar Éirinn* (History of Ireland), from the University College Dublin (UCD) Franciscan ‘A’ Manuscripts, reproduced by kind permission of UCD-OFM partnership. The order of results is again the same.

Numerical Comparison. To compare results objectively, it is necessary to convert them to a similar format. The *Huang* and *Mogh* methods produce images with varied foreground text intensities on a uniform background so could easily be compared to the ground truth images. However, the *RB* method produces images with smooth transitions between foreground text and a textured background; these were less comparable with the ground truth images. Therefore the solution proposed was to binarise all the results are using the adaptive document binarisation method of Gatos et al. [6]. These binary images were then compared to the manually created ground truth images. Three probability error metrics for each method were created over the full database: **FgError**, the probability that a pixel in the foreground text was classified as background, **BgError**, the probability that a background or bleed-through pixel was classified as foreground, and **TotError** the probability that any pixel in the image was misclassified. These were calculated as follows:

$$\begin{aligned}
 \text{FgError} &= \frac{1}{N} \sum_{GT(Fg)} |GT - B_Y| \\
 \text{BgError} &= \frac{1}{N} \sum_{GT(Bg)} |GT - B_Y| \\
 \text{TotError} &= \frac{1}{N} \sum_{GT} |GT - B_Y|
 \end{aligned} \tag{1}$$

Where GT is the ground truth, B_Y is the binarised restoration result, $GT(Fg)$ is the foreground region only of the ground truth image, similarly $GT(Bg)$ corresponds to the background region only, and N is the number of pixels in the image. The results obtained from applying the binarisation method (referred to as *Gatos*) to the degraded images, and then comparing these to the ground truth masks are also included in what follows. Figs. 2 and 3 show the BgError plotted against the FgError for each method over all 50 images, with overlaid ellipses defined by the mean error values and covariances between the two metrics. Comparisons of the BgError and FgError values between images can be misleading however, as these values depend on the relative size of the background and foreground regions in each image with respect to the text character size. For example an image that is mostly background, with small text, is likely to have a much smaller BgError value than an image with large text characters covering most of the image and proportionally less background region. It is more useful therefore to rank the performance of each method on each image, via the three error metrics (least probability of error to greatest), and then use these values to obtain an overall performance rank. Comparative error rankings between methods are shown in Table 1, where Opt refers to the optimised *Mogh* results, and each entry represents the percentage of times that the method listed vertically was ranked higher than the method listed horizontally. For instance *Mogh* (Opt) has a lower FgError than *Gatos* for 60% of the images. A further comparison of the ranks is shown in Fig. 4, where the percentage of images for which each rank was obtained is shown for each metric. Ranked Pairs Voting (RP) [13] was then used to obtain an overall rank for each of the methods. The mean error probabilities, and RP rank for all three methods are shown in Table 2.

Light Bleed-Through

sis. Metathesis. Apocope, $\delta\alpha\mu\omega\mu$, $\nu\epsilon\alpha\mu\omega\mu$,
 in aspiratione effecta $\kappa\gamma\omega\kappa\omega\varsigma$, in $\epsilon\pi\omega\epsilon$,
 crocus. Apocope, et ϵ , aspiratū. In Hebra-
 ica lingua $\gamma\lambda\eta$, $\lambda\alpha\beta\alpha\mu$, vertit in $\beta\alpha\mu$. i.

sis. Metathesis. Apocope, $\delta\alpha\mu\omega\mu$, $\nu\epsilon\alpha\mu\omega\mu$,
 in aspiratione effecta $\kappa\gamma\omega\kappa\omega\varsigma$, in $\epsilon\pi\omega\epsilon$,
 crocus. Apocope, et ϵ , aspiratū. In Hebra-
 ica lingua $\gamma\lambda\eta$, $\lambda\alpha\beta\alpha\mu$, vertit in $\beta\alpha\mu$. i.

sis. Metathesis. Apocope, $\delta\alpha\mu\omega\mu$, $\nu\epsilon\alpha\mu\omega\mu$,
 in aspiratione effecta $\kappa\gamma\omega\kappa\omega\varsigma$, in $\epsilon\pi\omega\epsilon$,
 crocus. Apocope, et ϵ , aspiratū. In Hebra-
 ica lingua $\gamma\lambda\eta$, $\lambda\alpha\beta\alpha\mu$, vertit in $\beta\alpha\mu$. i.

sis. Metathesis. Apocope, $\delta\alpha\mu\omega\mu$, $\nu\epsilon\alpha\mu\omega\mu$,
 in aspiratione effecta $\kappa\gamma\omega\kappa\omega\varsigma$, in $\epsilon\pi\omega\epsilon$,
 crocus. Apocope, et ϵ , aspiratū. In Hebra-
 ica lingua $\gamma\lambda\eta$, $\lambda\alpha\beta\alpha\mu$, vertit in $\beta\alpha\mu$. i.

Medium Bleed-Through

Domini piam loc
 - If se na an qrean
 - canaca upa eac
 - arsh'oneacdrin
 - shora glanpadoqe
 - da ndaizalam lei

Domini piam loc
 - If se na an qrean
 - canaca upa eac
 - arsh'oneacdrin
 - shora glanpadoqe
 - da ndaizalam lei

Severe Bleed-Through

Domini piam loc
 - If se na an qrean
 - canaca upa eac
 - arsh'oneacdrin
 - shora glanpadoqe
 - da ndaizalam lei

Domini piam loc
 - If se na an qrean
 - canaca upa eac
 - arsh'oneacdrin
 - shora glanpadoqe
 - da ndaizalam lei

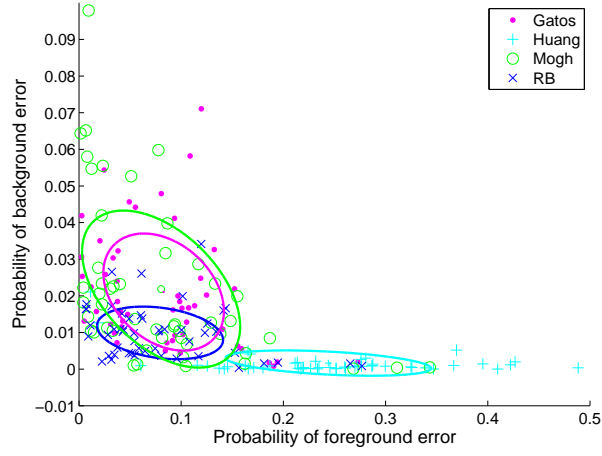
Domini piam loc
 - If se na an qrean
 - canaca upa eac
 - arsh'oneacdrin
 - shora glanpadoqe
 - da ndaizalam lei

Domini piam loc
 - If se na an qrean
 - canaca upa eac
 - arsh'oneacdrin
 - shora glanpadoqe
 - da ndaizalam lei

Domini piam loc
 - If se na an qrean
 - canaca upa eac
 - arsh'oneacdrin
 - shora glanpadoqe
 - da ndaizalam lei

Domini piam loc
 - If se na an qrean
 - canaca upa eac
 - arsh'oneacdrin
 - shora glanpadoqe
 - da ndaizalam lei

Fig. 1. Results on documents with varied bleed-through degradations (recto sides only shown). Order of images in each example from top to bottom: original recto crop, and results using Huang [8], Mogh [10] and RB [11]

**Fig. 2.** BgError vs FgError for all dataset**Table 1.** Pairwise Method Rank Comparison(%)

FgError	Gatos	Huang	Mogh/Opt	RB
Gatos	0	100	42/40	66
Huang	0	0	6/2	0
Mogh/Opt	58/60	94/98	0/0	58/50
RB	34	100	42/50	0
BgError	Gatos	Huang	Mogh/Opt	RB
Gatos	0	0	34/32	6
Huang	100	0	92/96	98
Mogh/Opt	66/68	8/4	0/0	28/24
RB	94	2	72/76	0
TotError	Gatos	Huang	Mogh/Opt	RB
Gatos	0	74	38/24	12
Huang	26	0	30/14	8
Mogh/Opt	62/76	70/86	0/0	26/26
RB	88	92	74/74	0

5 Discussion

The quantitative evaluations used were more objective than the visual comparisons, however the use of a binarisation technique on the clean image results was likely to favour images that have uniform background values, that is those from *Huang* and *Mogh*. *RB* however, maintains the image texture, and so was more likely to have misclassifications especially in images where the text was

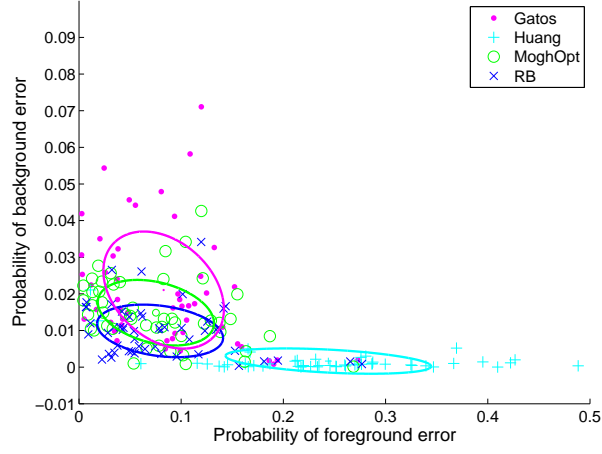


Fig. 3. BgError vs FgError for all dataset, with optimised *Mogh* results

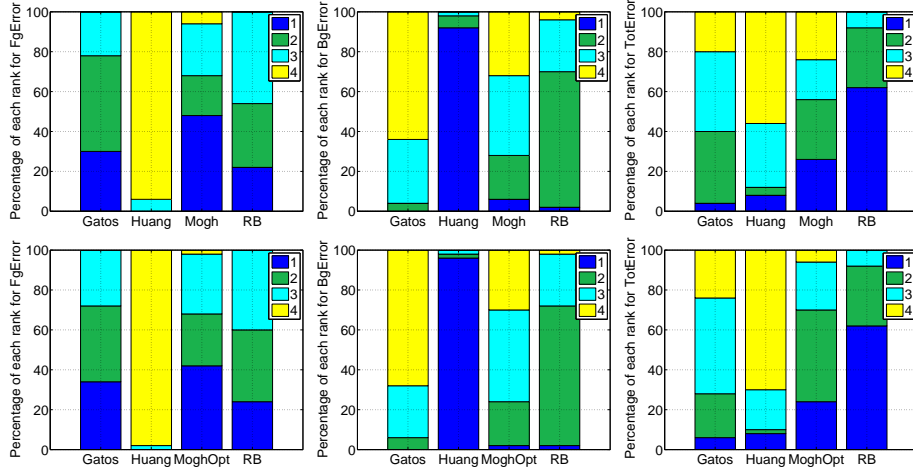


Fig. 4. Left to right: Percentage ranks for FgError, BgError, and TotError, with optimised *Mogh* results on the second row.

close in intensity to the background region, or where the background medium was highly textured. The choice of binarisation method helped to mitigate this; *Gatos* performed well itself on the degraded document images as can be seen in the rankings (Table 2), therefore it was capable of obtaining good estimates of foreground text from a noisy background. The comparison of the probability error metrics for each method (Figs. 2 & 3, and Table 2) highlights the visual observations already made. *Huang* performed the best in terms of BgError and

Table 2. Mean Error Probabilities and RP Ranks

	Gatos	Huang	Mogh/Opt	RB
Mean FgError	0.0828	0.2440	0.0804/0.0753	0.0793
RP FgRank	2	4	1	3
Mean BgError	0.0210	0.0016	0.0219/0.0149	0.0099
RP BgRank	4	1	3	2
Mean TotError	0.0304	0.0424	0.0302/0.0244	0.0216
RP TotRank	3	4	2	1

hence in terms of full bleed-through removal, however as a lot of foreground text was removed the mean FgError was the highest. The *Mogh* mean error values improved significantly when the manually optimised smoothing parameters were used, this is also clearly highlighted in the graphs (Figs. 2 and 3) as the points are much more closely grouped in the optimised graph. The pairwise rank comparisons were only slightly altered with the optimised smoothing parameter, and the overall rankings were unaffected. The fact that the *RB* performed best in terms of the TotErr, but was ranked third for the FgError and second for BgError emphasises the differences in results obtained from the other methods. *Huang* uses a relatively harsh classification which allows for no ambiguity in the results, and while *Mogh* creates a smooth result, since the final results are on a plain background, this makes any remaining artefacts much more noticeable. These differences however result from different aims when creating a bleed-through removal solution; the *Mogh* and *Huang* results would be suitable as inputs for optical character recognition systems to improve recognition compared to the degraded images, and also would be useful to improve compression for storage since background texture and noise has been removed. *RB* however, would not be suitable for these applications as the resulting images aim to leave as much of the original document intact as possible, and are targeted at researchers studying the content contained within them. Knowing these differences a priori was essential in obtaining an objective comparison between the methods.

6 Conclusion

A bleed-through degraded document image database has been presented and its usefulness demonstrated by comparing the results of three non-blind bleed-through removal techniques against manually created ground truth foreground masks. Numerical comparisons between different methods will always be difficult due to the variability in the format of results produced. Binary masks were therefore created as ground truth, and the results of each method were binarised to ensure that numerical comparisons were as objective as possible. The overall ranking of results showed that the while *Huang* performed best in terms of complete bleed-through removal, and *Mogh* was ranked first in terms of foreground text preservation, *RB* performed best in terms of the overall error.

Acknowledgments. The authors would like to thank Prof. Pádraig Ó Macháin from ISOS for his assistance. This research has been funded by the Irish Research Council for Science, Engineering, and Technology ‘Embark’ Initiative.

References

1. Burgoyne, J.A., Devaney, J., Pugin, L., Fujinaga, I.: Enhanced bleedthrough correction for early music documents with recto-verso registration. In: *Int. Conf. Music Inform. Retrieval*. pp. 407–412. Philadelphia, PA (2008)
2. Castro, P., Almeida, R.J., Pinto, J.R.C.: Restoration of double-sided ancient music documents with bleed-through. In: Rueda, L., Mery, D., Kittler, J. (eds.) *CIARP, LNCS*, vol. 4756, pp. 940–949. Springer Berlin/Heidelberg (2007)
3. Drira, F., Le Bourgeois, F., Emptoz, H.: Restoring ink bleed-through degraded document images using a recursive unsupervised classification technique. In: Bunke, H., Spitz, A. (eds.) *DAS, LNCS*, vol. 3872, pp. 38–49. Springer Berlin / Heidelberg (2006)
4. Dubois, E., Pathak, A.: Reduction of bleed-through in scanned manuscript documents. In: *IS&T Image Process., Image Quality, Image Capture Syst. Conf.* vol. 4, pp. 177–180. Montreal, Canada (2001)
5. Estrada, R., Tomasi, C.: Manuscript bleed-through removal via hysteresis thresholding. In: *10th Int.l Conf. Doc. Anal. and Recogn.* pp. 753–757. Barcelona, Spain (2009)
6. Gatos, B., Pratikakis, I., Perantonis, S.J.: Adaptive degraded document image binarization. *J. Pattern Recogn.* 39(3), 317–327 (2006)
7. Huang, Y., Brown, M.S., Xu, D.: A framework for reducing ink-bleed in old documents. In: *IEEE Conf. Comput. Vis. Pattern Recogn.* pp. 1–7. Anchorage, AK (2008)
8. Huang, Y., Brown, M.S., Xu, D.: User-assisted ink-bleed reduction. *IEEE Trans. Image Process.* 19(10), 2646–2658 (2010)
9. Moghaddam, R.F., Cheriet, M.: Low quality document image modeling and enhancement. *Int. J. Doc. Anal. Recogn.* 11(4), 183–201 (2009)
10. Moghaddam, R.F., Cheriet, M.: A variational approach to degraded document enhancement. *IEEE Trans. Pattern Anal. Mach. Intell.* 32(8), 1347–1361 (2010)
11. Rowley-Brooke, R., Kokaram, A.: Bleed-through removal in degraded documents. In: *SPIE: Doc. Recogn. Retrieval Conf.* San Francisco, CA (2012)
12. Sauvola, J., Pietikäinen, M.: Adaptive document image binarization. *J. Pattern Recogn.* 33(2), 225–236 (2000)
13. Tideman, T.N.: Independence of clones as a criterion for voting rules. *J. Soc. Choice Welf.* 4(3), 185–206 (1987)
14. Tonazzini, A.: Color space transformations for analysis and enhancement of ancient degraded manuscripts. *J. Pattern Recogn. Image Anal.* 20(3), 404–417 (2010)
15. Tonazzini, A., Bedini, L., Salerno, E.: Independent component analysis for document restoration. *Int. J. Doc. Anal. Recogn.* 7(1), 17–27 (2004)
16. Tonazzini, A., Salerno, E., Bedini, L.: Fast correction of bleed-through distortion in grayscale documents by a blind source separation technique. *Int. J. Doc. Anal. Recogn.* 10(1), 17–25 (2007)
17. Wolf, C.: Document ink bleed-through removal with two hidden markov random fields and a single observation field. *IEEE Trans. Pattern Anal. Mach. Intell.* 32(3), 431–447 (2010)